

# Thermodynamic Analysis of Organic Rankine Cycle using EES Solver

M. Tech.Scholar Anshul Dhamecha      Prof. Pooja Tiwari

Department of Mechanical Engineering  
SIRT, Jabalpur, MP, India

**Abstract** - The development of the world today has largely been achieved through the increasingly efficient and extensive use of various forms of energy. Over the past decades, the growth in energy consumption around the world has shown that fossil fuel energy source alone will not be capable of meeting future energy demands. The purpose of this study is to parametrically analyze and compare the first law efficiency, second law efficiency and turbine size factor of the ORCs using R143a, R600a, R134a and RC318 as working fluids. A computer program in Engineering Equation Solver (EES) has been developed to simulate the thermodynamic performance of the tested working fluids under various heat source temperatures.

**Keywords**- EDM, Taguchi Method, Optimization, ANOVA.

## I. INTRODUCTION

With the increase in fossil fuel consumptions, more and more industrial activities produce increasing amount of waste heat. Energy generated as a result of industrial activities that are not practically utilized is referred to as industrial waste heat. Several studies have shown that the specific amount of industrial waste heat is poorly measured, it is estimated that 25 to 55% of the input energy in industries are actually used while the remaining are discharged as waste heat [1]. While it is almost impossible to avoid waste heat losses from industrial activities, some facilities and heat recovery technologies can be put in place to reduce these waste heats by improving equipment efficiency and energy utilization.

The extraction of energy from waste heat, turbine exhaust, solar energy and biomass energy is becoming a popular means of generating alternative energy for most industries. Low grade heat sources can be converted into electrical power and these can be achieved using an ORC system. The basic principles of the ORCs are very much like those of the conventional Rankine cycle. However, the main difference is that the ORC uses an organic working fluid which has a higher vapor pressure and lower boiling point compared to water.

These properties of organic fluids boost the cycle efficiency of the ORCs considerably compared to the conventional Rankine cycle. There have been several successful installations of the ORCs around the world and more research is still being carried out to improve the ORC system. The increase in the energy consumption by burning of fossil fuel has led to several conflicts around the world, global warming and environmental pollution such as soil, water, air and acid rain pollution. Besides the adverse environmental effects, the prices of fossil fuels are not consistent but usually going up most of the time.

Petroleum and natural gas and coal are fossil fuels and are non-renewable. Several countries today have been investing money to get new and efficient energy technologies that are alternative for fossil fuels to generate power. Low grade heat is largely available in renewable energy sources and in industrial waste. Utilizing this type of sustainable energy could help reduce the use of non-renewable energy, thus reducing the environmental impacts of non-renewable energy sources. Development of efficient and effective technologies is required to generate useful work by using these low grade heat sources.

An ORC is a suitable means of carrying out this purpose. The ORC works with a high molecular mass organic working fluid with the characteristic of having a phase change of liquid to vapour occurring at a temperature which is lower than the phase change of water to steam for a given pressure. The recovery of low grade heat can be achieved using organic fluids. These low grade heat sources can be from biomass energy, solar energy, geothermal energy and industrial waste. The ORC converts the low grade heat into work and finally into electricity.

## II. SYSTEM MODELING

To aid in analysis of engineering problem it is necessary to realize the Physical model in a mathematical model. To do this, we first write state point equations of thermodynamic properties and then develop a polynomial for thermodynamic properties with the help of software or, directly taken from the reference. Therefore this chapter involves the description of physical model, mass, and energy balance, assumptions, state point equations and thermodynamic properties. We will calculate and compare thermal efficiency, generating capacity, etc. of

power systems, namely AC-ORC under the same heat source conditions.

### III. SYSTEM DESCRIPTION

The ORC investigated in this paper is shown in Fig. 1. It consists of four different processes: process 1-2 (expansion through turbine), process 2-3 (heat rejection in condenser), process 3-4 (pressurized in pump), and process 4-1 (heat addition in evaporator).

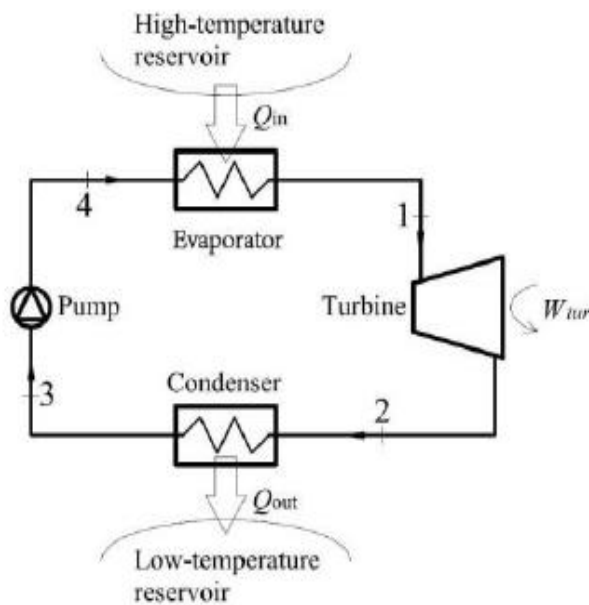


Fig. 1 Schematic diagram of the organic Rankine cycle

The analysis is based on the following as assumptions:

- The system is operating under steady-state condition,
- No undesired pressure drop and heat loss occur in the system,
- Working fluid at the evaporator and condenser exits is saturated, and
- Isentropic efficiencies for the turbine and pump.

### IV. SIMULATION ASSUMPTIONS IN THE ANALYSES

The followings are the assumptions used in the study

1. The pressure drops in the heat exchangers are neglected.
2. The expander and pump's isentropic efficiencies are considered to be 0.9.
3. Condensing temperature  $T_{Cond.} = 28^{\circ}C$
4. Evaporating temperature  $T_{Evap.} = 120^{\circ}C$ .
5. The mass flow rates of the hot and cold fluid in the internal heat exchanger are assumed to be the same.
6. There is no temperature increase or decrease between the evaporator exit temperature and the expander inlet temperature.

### V. MATHEMATICAL MODELLING

Modeling equations are developed and programmed in Engineering Equation Solver (EES). The computational modeling is based on the following general assumptions. The system is considered under steady state. Friction, heat loss, changes in kinetic and potential energy is neglected. The pressure drops in heat exchangers and tubes are negligible. The working fluid in the VCC enters the compressor at saturated vapor state and exits the condenser at saturated liquid state. Expansion process in the VCC is adiabatic process. The designed condensation temperature of the AC subsystem is not affected by the ORC subsystem. The working fluid in the ORC exits the condenser at saturated liquid state and enters the turbine at saturated vapor state.

$$\text{Mass balance: } \sum_{in} \dot{m} = \sum_{out} \dot{m}$$

$$\text{Energy balance: } \dot{Q} - \dot{w} = \sum_{out} \dot{m}h - \sum_{in} \dot{m}h$$

The net power output of the ORC system ( $W_{net}$ ) is calculated by Eqs

$$\begin{aligned} W_{net} &= W_{turbine} - W_{pump} \\ W_{pump} &= \dot{m} (h_{4s} - h_3) / \eta_{pump} \\ W_{turbine} &= \dot{m} (h_1 - h_{2s}) \eta_{turbine} \end{aligned}$$

Where,  $W_{pump}$  is the power consumed by the pump;  $h_{4s}$  is the isentropic specific enthalpy of working fluid at the pump exit;  $\eta_{pump}$  is the pump isentropic efficiency;  $W_{tur}$  is the turbine power output;  $h_{2s}$  is the is entropic specific enthalpy of working fluid at the turbine exit;  $\eta_{tur}$  is the turbine isentropic efficiency. The first and second law efficiencies of the ORC ( $\eta_I$  and  $\eta_{II}$ ) are defined by Eqs.

$$\begin{aligned} \eta_I &= W_{net} / Q_{in} \\ \eta_{II} &= W_{net} / [Q_{in} (1 - T_o / T_m)] \end{aligned}$$

where,  $T_o$  is the ambient temperature;  $T_m$  is the mean heat source temperature;  $Q_{in}$  is the heat transfer rate in the evaporator. The turbine size factor (TSF), which is proportional to actual turbine size is given by.

$$TSF = \frac{\sqrt{V_2}}{\Delta H_{is}^{1/4}}$$

Where,  $V_2$  is volumetric flow rate at turbine exit, and  $\Delta H_{is}$  is the isentropic enthalpy difference in the turbine.

### VI. RESULTS AND DISCUSSION

#### 1. Effect of Heat Source Temperature

The purpose of this study is to parametrically analyse and compare the first law efficiency, second law efficiency and turbine size factor of the ORCs using R143a, R600a, R134a and RC318 as working fluids. A computer program in Engineering Equation Solver (EES) has been developed to simulate the thermodynamic performance of the tested working fluids under various heat source temperatures.

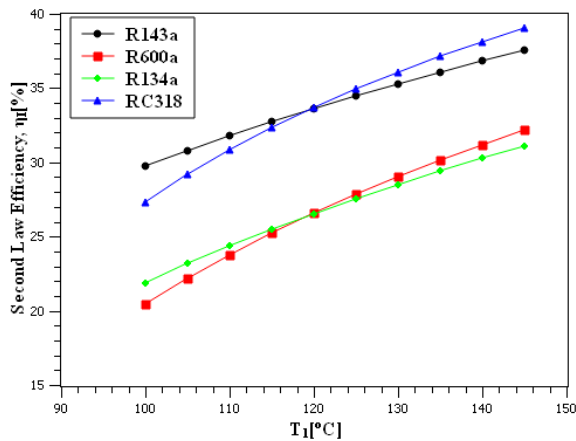


Fig. 2 Variation of second law efficiency.

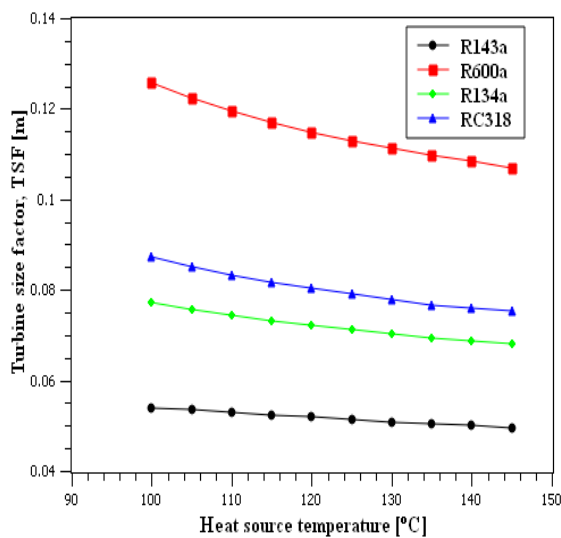


Fig. 3 Variation of turbine size factor vs heat source temperature.

Fig. 2 shows the effect of the heat source temperature on the second law efficiency of the ORC. It is found that with different working fluids, the influences of the heat source temperature on the first law efficiency are similar. It shows that the first law thermal efficiency increases monotonically with the increase in heat source temperature. With the TET rising from 100 to 145 °C, the first law efficiencies approximately increase by 39.34 % for R143a, 73.53 % for R600a, 56.76 % for R134a and 57.6 % for RC318. RC318 obtains the highest thermal efficiency, followed by R143a, R600a and R134a which shows relatively poor performance.

Fig. 3 illustrates the effects of the TET on the turbine size factor of the ORC. It is seen that the turbine size factor always decreases as the heat source increases. For the conditions under consideration, small size factors are obtained for R143a at high TETs. R600a requires the largest size parameter due to the very low evaporation pressure. Overall, R143a has the lowest turbine size parameter at all the TETs.

## 2. Effect of Turbine Inlet Temperature

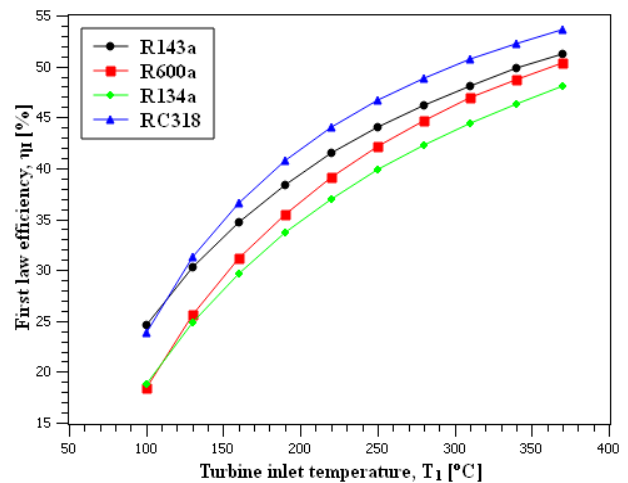


Fig. 4 Variation of first law efficiency vs turbine inlet temperature

Fig. 4 shows the effect of turbine inlet temperature on the first law efficiency of the ORC. It is found that with different working fluids, the influences of the heat source temperature on the first law efficiency are similar. It shows that the first law thermal efficiency increases monotonically with the increase in turbine inlet temperature. With the TET rising from 100 to 370°C, the first law efficiencies approximately increase for R143a, R600a, R134a and for RC318. RC318 obtains the highest thermal efficiency, followed by R143a, R600a and R134a which shows relatively poor performance.

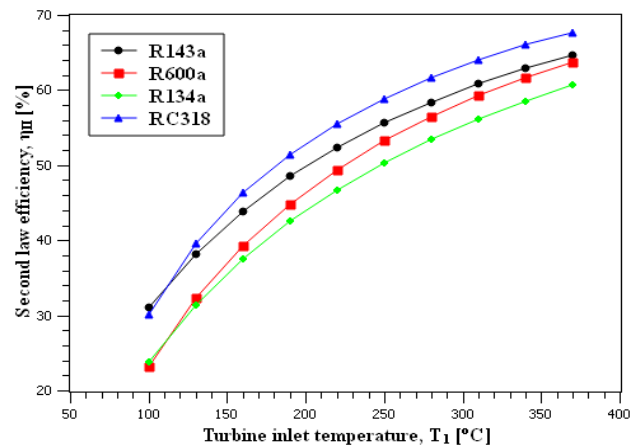


Fig. 5 Variation of second law efficiency vs turbine inlet temperature.

The variation of second law efficiency versus the turbine inlet temperature is shown in Fig. 5. It can be seen that the second law efficiencies increase with the turbine inlet temperature. With the turbine inlet temperature rising from 100 to 370°C, the second law efficiencies approximately increase for R143a, R600a, R134a and for RC318. RC318 obtains the highest thermal efficiency,

followed by R143a, R600a and R134a which shows relatively poor performance.

Fig. 6 illustrates the effects of the TET on the turbine size factor of the ORC. It is seen that the turbine size factor always decreases as the TET increases. For the conditions under consideration, small size factors are obtained for R143a at high TETs. R600a requires the largest size parameter due to the very low evaporation pressure. Overall, R143a has the lowest turbine size parameter at all the TETs.

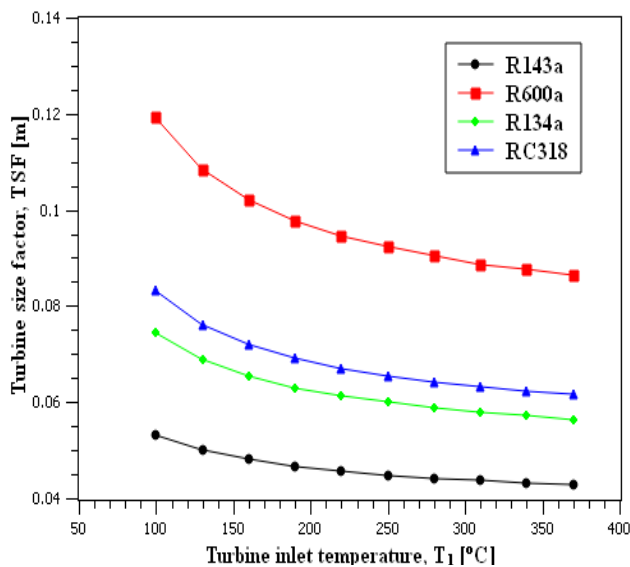


Fig. 6 Variation of turbine size factor vs turbine inlet temperature.

### 3. Effect of Pinch Point Temperature Difference

The purpose of this study is to parametrically analyze and compare the first law efficiency, second law efficiency and turbine size factor of the ORCs using R143a, R600a, R134a and RC318 as working fluids. A computer program in Engineering Equation Solver (EES) has been developed to simulate the thermodynamic performance of the tested working fluids under various pinch point temperature difference. Fig. 7 shows the effect of pinch point temperature difference on the first law efficiency of the ORC.

It is found that with different working fluids, the influences of the pinch point temperature difference on the first law efficiency are similar. It shows that the first law thermal efficiency decreases monotonically with the increase in pinch point temperature difference. With the pinch point temperature difference rising from 10 to 28°C, the first law efficiencies approximately decreases for R143a, R600a, R134a and for RC318. R143a obtains the highest thermal efficiency, followed by RC318, R134a and R600a which shows relatively poor performance.

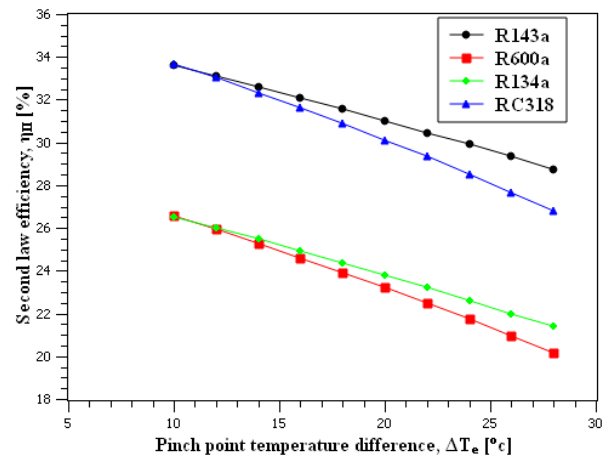


Fig. 8 Variation of second law efficiency vs pinch point temperature difference.

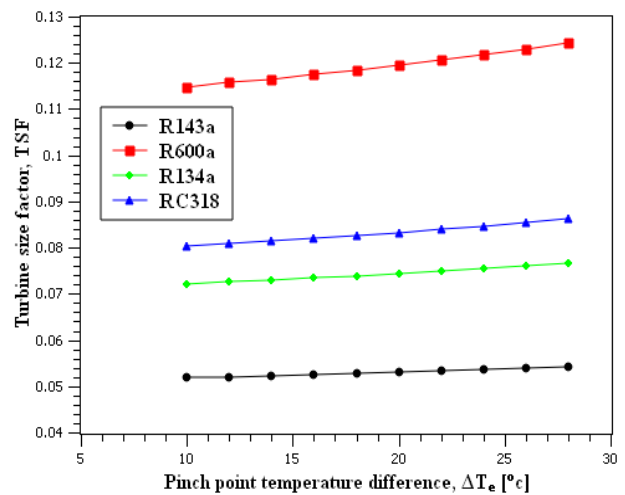


Fig. 9 Variation of turbine size factor vs pinch point temperature difference.

Fig. 8 shows the effect of pinch point temperature difference on the second law efficiency of the ORC. It is found that with different working fluids, the influences of the pinch point temperature difference on the first law efficiency are similar. It shows that the first law thermal efficiency decreases monotonically with the increase in pinch point temperature difference.

With the pinch point temperature difference rising from 10 to 28°C, the first law efficiencies approximately decreases for R143a, R600a, R134a and for RC318. R143a obtains the highest thermal efficiency, followed by RC318, R134a and R600a which shows relatively poor performance. Fig. 9 illustrates the effects of the TET on the turbine size factor of the ORC. It is seen that the turbine size factor always increases as the TET increases. For the conditions under consideration, small size factors are obtained for R143a at high TETs. R600a requires the largest size parameter due to the very low evaporation pressure. Overall, R143a has the lowest turbine size parameter at all the TETs.

#### 4. Effect of Turbine Efficiency

The purpose of this study is to parametrically analyse and compare the first law efficiency, second law efficiency and turbine size factor of the ORCs using R143a, R600a, R134a and RC318 as working fluids. A computer program in Engineering Equation Solver (EES) has been developed to simulate the thermo dynamic performance of the tested working fluids under various turbine efficiency.

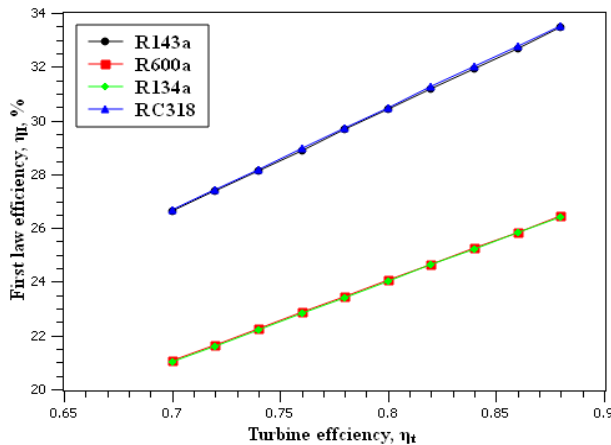


Fig. 10 Variation of first law efficiency vs turbine efficiency

Fig. 10 shows the effect of turbine efficiency on the first law efficiency of the ORC. It is found that with different working fluids, the influences of the turbine efficiency on the first law efficiency are similar. It shows that the first law thermal efficiency increases monotonically with the increase in turbine efficiency. With the turbine efficiency rising from 70 to 88%, the first law efficiencies approximately increases for R143a, R600a, R134a and for RC318. R143a and RC318 obtain the highest thermal efficiency, followed by R134a and R600a which shows relatively poor performance.

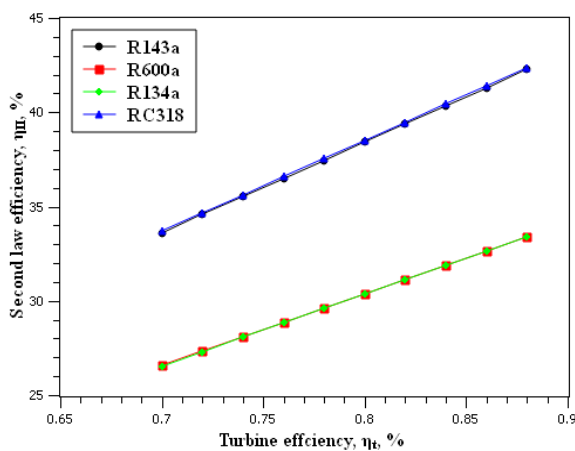


Fig. 11 Variation of second law efficiency vs turbine efficiency.

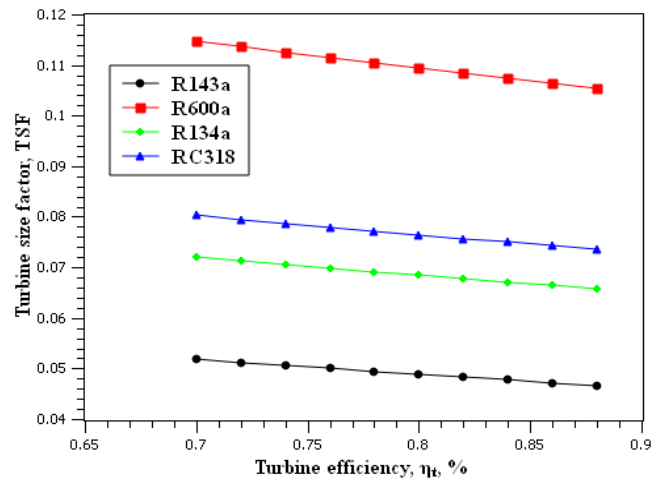


Fig. 12 Variation of turbine size factor vs turbine efficiency.

Fig. 11 shows the effect of turbine efficiency on the second law efficiency of the ORC. It is found that with different working fluids, the influences of the turbine efficiency on the second law efficiency are similar. It shows that the second law thermal efficiency increases monotonically with the increase in turbine efficiency. With the turbine efficiency rising from 70 to 88%, the second law efficiencies approximately increases for R143a, R600a, R134a and for RC318. R143a and RC318 obtain the highest thermal efficiency, followed by R134a and R600a which shows relatively poor performance.

Fig. 4.12 illustrates the effects of the TET on the turbine size factor of the ORC. It is seen that the turbine size factor always decreases as the TET increases. For the conditions under consideration, small size factors are obtained for R143a at high TETs. R600a requires the largest size parameter due to the very low evaporation pressure. Overall, R143a has the lowest turbine size parameter at all the TETs.

#### VII. CONCLUSION

1. It is found that with different working fluids, the influences of the heat source temperature on the first law and second efficiency are similar. It shows that the first law and second law thermal efficiency increases monotonically with the increase in heat source temperature. With the heat source temperature rising from 100 to 145 °C, the first law and second law efficiencies approximately increases for all working fluids. RC318 obtains the highest thermal efficiency, followed by R143a, R600a and R134a which shows relatively poor performance.
2. It is seen that the turbine size factor always decreases as the heat source increases. For the conditions under consideration, small size factors are obtained for R143a at high TETs. R600a requires the largest size parameter due to the very low evaporation pressure. Overall, R143a has the lowest turbine size parameter at all the TETs.

3. It is found that with different working fluids, the influences of the turbine inlet temperature on the first law and second law efficiency are similar. It shows that the first law and second law thermal efficiency increases monotonically with the increase in turbine inlet temperature. With the TET rising from 100 to 370°C, the first law and second law efficiencies approximately increases for R143a, R600a, R134a and for RC318. RC318 obtains the highest thermal efficiency, followed by R143a, R600a and R134a which shows relatively poor performance.
4. It is seen that the turbine size factor always decreases as the TET increases. For the conditions under consideration, small size factors are obtained for R143a at high TETs. R600a requires the largest size parameter due to the very low evaporation pressure. Overall, R143a has the lowest turbine size parameter at all the TETs.
5. It is found that with different working fluids, the influences of the pinch point temperature difference on the first law and second law efficiency are similar. It shows that the first law thermal efficiency decreases monotonically with the increase in pinch point temperature difference. With the pinch point temperature difference rising from 10 to 28°C, the first law and second law efficiencies approximately decreases for R143a, R600a, R134a and for RC318. R143a obtains the highest thermal efficiency, followed by RC318, R134a and R600a which shows relatively poor performance.
6. It is seen that the turbine size factor always increases as the TET increases. For the conditions under consideration, small size factors are obtained for R143a at high TETs. R600a requires the largest size parameter due to the very low evaporation pressure. Overall, R143a has the lowest turbine size parameter at all the TETs.
7. It is found that with different working fluids, the influences of the turbine efficiency on the first law and second law efficiency are similar. It shows that the first law thermal efficiency increases monotonically with the increase in turbine efficiency. With the turbine efficiency rising from 70 to 88%, the first law and second law efficiencies approximately increases for R143a, R600a, R134a and for RC318. R143a and RC318 obtain the highest thermal efficiency, followed by R134a and R600a which shows relatively poor performance.
8. It is seen that the turbine size factor always decreases as the TET increases. For the conditions under consideration, small size factors are obtained for R143a at high TETs. R600a requires the largest size parameter due to the very low evaporation pressure. Overall, R143a has the lowest turbine size parameter at all the TETs.

## REFERENCES

- [1] Virang H Oza, Nilesh M Bhatt, Optimization of Ammonia-Water Absorption Refrigeration System using Taguchi Method of Design of Experiment, International Journal of Mechanics and Solids, 13(2), 111-126, 2018.
- [2] F. H. Napitupulu (2017), A Preliminary Study on Designing and Testing of an Absorption Refrigeration Cycle Powered by Exhaust Gas of Combustion Engine, IOP Conf. Series: Materials Science and Engineering, 180.
- [3] Tushar Charate (2017), A Review of Absorption Refrigeration in Vehicles using Waste Exhaust Heat, International Journal of Scientific & Engineering Research, 8(3), 65-67.
- [4] Ezaz Ahmad Ansari (2015), Study of Ammonia Water Vapour Absorption Refrigeration Chiller Run by Solar Thermal Energy, International Journal of Scientific Engineering and Research, 5(7), 385-388.
- [5] Aman Shukla, C.O.P Derivation and Thermodynamic Calculation of Ammonia-Water Vapor Absorption Refrigeration System, International Journal of Mechanical Engineering and Technology, 6(5), 72-81, 2015.
- [6] Rahul Singh and Dr. Rajesh Kumar (2014), Theoretical Analysis of  $\text{NH}_3\text{-H}_2\text{O}$  Refrigeration System Coupled With Diesel Engine: A Thermodynamic Study, IOSR Journal of Mechanical and Civil Engineering, 11(3), 29-36.
- [7] Sachin Kaushik, Dr. S. Singh, Thermodynamic Analysis of Vapor Absorption Refrigeration System and Calculation of COP, International Journal for Research in Applied Science and Engineering Technology, 2(2), 73-80, 2014.
- [8] Janardhanan.k, J. vishagan. V, U. Gowtham, A. Pokhrel, D. kumar, Jaypal, J. Prakash, A. Sivasubramanian, and Dr.G. Arunkumar, "Using engine exhaust gas as energy source for an absorption refrigeration system", International journal of Scientific Research, vol. 3, no. 11, 2014.
- [9] J. Yadav and B. R. Singh, "Experimental set up of air conditioning system in automobile using exhaust energy", S-jpset, vol. 5, 2014.
- [10] Ahmed Ouadha, Youcef El-Gotni (2013), Integration of an ammonia-water absorption refrigeration system with a marine Diesel engine: A thermodynamic study, The 3rd International Conference on Sustainable Energy Information Technology, Procedia Computer Science, 19, 754 – 761.
- [11] C. V. Vazhappilly, T. Tharayil, A.P. Nagarajan, "Modeling and experimental analysis of generator in vapor absorption refrigeration system", Journal of Engineering Research and Application, vol. 3, no. 5, 2013.
- [12] M. Pavoodath, "Absorption ac in vehicles using exhaust gas", International Conference on Automation, Control and Robotics, 2012.

- [13] K. S. AlQdah, "Performance and evaluation of aqua ammonia auto air conditioner system using exhaust waste energy", *Energy Procedia*, vol. 6, 2011.
- [14] Satish Raghuvanshi, Govind Maheshwari, Analysis of Ammonia –Water ( $\text{NH}_3\text{-H}_2\text{O}$ ) Vapor Absorption Refrigeration System based on First Law of Thermodynamics, *International Journal of Scientific & Engineering Research*, 2(8), 1-7, 2011.
- [15] Manzela, S. M. Hanriot, L. C. Gomez, and J. R. Sodre, "Using engine exhaust gas as energy source for an absorption refrigeration system", *Applied Energy*, vol. 87, 2010.